ELSEVIER

Biophysical Chemistry 96 (2002) 1–14

Biophysical Chemistry

www.elsevier.com/locate/bpc

The nature of the receptor site for the reversible K^+ channel blocking by aminopyridines

Camelia Muñoz-Caro*, Alfonso Niño

Grupo de Química Computacional, Escuela Superior de Informática, Universidad de Castilla-La Mancha, Paseo de la Universidad 4, 13071 Ciudad Real, Spain

Received 20 December 2001; received in revised form 21 December 2001; accepted 2 January 2002

Abstract

This work presents a theoretical study aimed at the identification of the receptor site for the blocking of the voltage dependent K^+ channels by protonated aminopyridines. Thus, the density functional theory (DFT) at the B3LYP/6-311 G (d,p) level is applied, both in vacuum and in solution, to a series of active (protonated) compounds: 2-aminopyridine, 3-aminopyridine, 4-aminopyridine, 3,4-diaminopyridine, and 4-aminoquinoleine. Analysis of the X-ray structure of the α-subunit of the channel shows that charged aminopyridines can interact electrostatically with a glutamic acid residue in the outside of the pore, or through a cation–π interaction in the inside. To test both possibilities, model complexes are built using as nucleophiles a carboxylic group and an ethylene molecule, respectively. The three-dimensional electrostatic potential distribution of the protonated aminopyridines shows that an approaching nucleophile will be oriented toward the N–H (protonated) bond. Interaction with the carboxylic residue leads to a proton transfer, with the aminopyridine–carboxylic acid linked by a hydrogen bond. The observed breaking of the equivalence of the Laplacian of the charge density, the relative energy variation for the complexes, and the interaction with only one of the carboxylic residues in the fourfold α-subunit of the K^+ channel are not compatible with the observed in vitro activity variation of aminopyridines. On the other hand, the study on the ethylene complexes shows, in vacuum and solution, a cation–π interaction, clearly characterized by the atoms in molecules (AIM) theory. The variation of relative energy in solution is very small, but approaches the variation of in vitro activity. Our results, the pharmacophoric characteristics of aminopyridines, and the analysis of the three-dimensional internal structure of the K^+ channel α-subunit suggest two putative receptor sites. One is formed by the four Thr–Thr–Val chains conforming the entrance to the narrow part of the inner K^+ channel. The other is defined by four Thr residues within the pore.

Keywords: K^+ channel blocking; Theoretical modelling; Aminopyridines; Receptor site

1. Introduction

Aminopyridines are bioactive *N*-heterocyclic tertiary amines that inactivate the voltage-dependent K^+ channels [1–3]. Thus, the efflux of intracellular K^+ is blocked, leading to the maintenance of the pre-synaptic action potential, and consequently, increasing the nerve signal [2]. Due to their ability to facilitate nerve transmission, aminopyridines have been applied to reverse anesthesia and muscle relaxation [3]. In addition, they

*Corresponding author. Tel.: +34-926-295362; fax: +34-926-295354.

E-mail address: quimcom@uclm.es (C. Muñoz-Caro).

0301-4622/02/$ - see front matter
PII: S0301-4622(02)00002-9

have been proposed as drugs for the treatment of multiple sclerosis [4], myasthenia gravis [5], spinal cord injuries [6], botulism [7] and Alzheimer's disease [8].

Aminopyridines are weak bases, $pK_a \simeq 9.0$, and thus they can exist in neutral or cationic (protonated) form at physiological pH. Both the experimental [9–14] and theoretical evidence [15,16] agrees in that a positive charge, a consequence of protonation, and one or more amine groups, suitable for hydrogen bonding, constitute the pharmacophoric characteristics of aminopyridines. However, the mechanism by which protonated aminopyridines (APH^+) inactivate the K^+ channel, as well as the physical nature of the receptor site is not yet known.

The K^+ channel is a tetramer with four-fold rotational symmetry (almost a C_4 point group symmetry) about a central pore [17]. Each subunit has two-transmembrane α-helices. One of the α-helices of each subunit faces the pore while the other faces the lipid membrane [17]. The overall structure resembles an inverted teepee or cone, with the narrow end towards the cytoplasmic side. This structure defines the α subunit of the channel. The cytoplasmic (T1) domain of each a subunit acts as a docking platform for a β subunit. This β subunit is a tetramer of oxidoreductase proteins, and the full ensemble is arranged again in a four-fold C_4 structure [18]. This $T1_4\beta_4$ section resembles a base for the pore in the cytoplasmic side.

From the cytoplasmic side, the K^+ channel is blocked by quaternary ammonium cations such as tetraethylammonium (TEA), and by the NH_2 terminal peptide segment from the channel itself. X-Ray analysis shows that the central pore in the $T1_4\beta_4$ assembly is narrow (approx. 4 Å) and positively charged [18]. Thus, accessing the pore through that hole is not possible for the TEA or the inactivation peptide. On the basis of mutant cycle analysis, the experimental evidence [18] shows that the transmembrane pore communicates with the cytoplasm through four lateral negatively charged openings in the T14β4 complex.

X-Ray data [17] shows that the pore is conformed as a tunnel approximately 45 Å in length. From the intracellular side, a portion of the tunnel, 18 Å in length, ends in a cavity of approximately 10 Å in width. In this zone, a K^+ ion can move and be still hydrated. This zone is large enough to admit quaternary ammonium cations, such as TEA or tetrabutylammonium (TBA), as well as the inactivation peptide [19]. From the cavity to the extracellular region, the tunnel is much narrower, and a K^+ cation needs to lose its solvating water to enter.

A recent X-ray diffraction study has been carried out to determine the receptor site for the inactivation peptide and quaternary amine inhibitors of Shaker-type K^+ channels [19]. The data are consistent with the view that TBA and the first amino acids of the inactivation peptide bind somewhere into the large central cavity. The study also clearly shows that the inner linen of the pore is mainly formed by hydrophobic amino acids, whereas out the pore, in the cytoplasmic side, acidic amino acids are found.

Since the positive charge is a pharmacophoric requirement in aminopyridines, it has been proposed that ionic (cation–anion) interactions play a prominent role in stabilizing the APH^+–receptor complex [15]. However, in the light of the present structural knowledge of the K^+ channel, this hypothesis seems less plausible. The role played by the positive charge, and where and how aminopyridines bind in the pore to reversibly block the K^+ channel are still unresolved.

In this work, we present a theoretical study aimed at shedding some light on the physical nature and placement of the receptor site for APH^+ in the K^+ channel. As in our previous study [16], the following series of protonated compounds (in order of increasing in vitro activity [12]) are considered: 2-aminopyridine (2-APH^+), 3-aminopyridine (3-APH^+), 4-aminoquinoleine (4-AQH^+), 4-aminopyridine (4-APH^+), and 3,4-diaminopyridine (3,4-$DiAPH^+$), see Fig. 1. From the X-ray tridimensional structure of the tetrameric α-subunit of the KcsA K^+ channel [19], the distribution and kind of possible receptor sites with the needed nucleophilic character are determined. The relative orientation of an interacting nucleophilic group with the APH^+ is considered from the three-dimensional distribution of the molecular electrostatic potential. Supermolecular

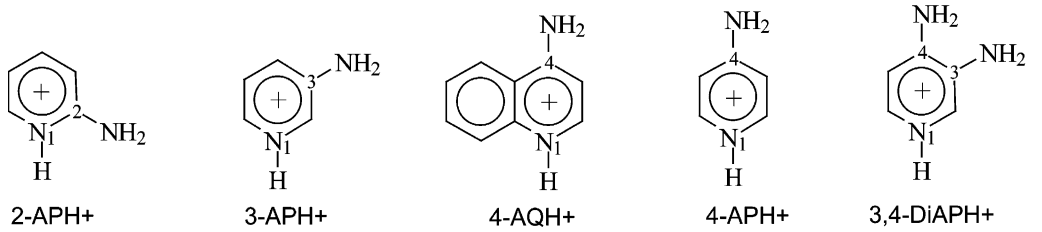

Fig. 1. Structure and numbering convention for the series of protonated aminopyridines (in order of increasing in vitro activity) considered in this work.

models corresponding to ionic and cation–π interactions with the receptor are developed and analyzed. Since, in the large central cavity of the pore, aminopyridines can be partially hydrated, the APH^+ complexes are described in vacuum and solution. A comparison of both cases provided a picture of their behavior in biological medium. Finally, two possible receptor sites are proposed.

2. Theoretical methods

All molecular data have been obtained at the correlated level, using the density functional theory (DFT) by means of the B3LYP method. The hybrid B3LYP method is used since it leads to reliable structures and harmonic vibrational frequencies for equilibrium structures [20–22]. Together with the B3LYP method, we have used the triple split valence plus polarization 6-311G(d,p) basis set, which has been developed at the correlated level [23]. It has been shown that this basis is able to reproduce accurately structures and anharmonic vibrations [24–26].

To have a realistic description of the molecular behavior in aqueous solution (dielectric constant 78.39) the solvent effect is considered by means of the Polarizable Continuum Model (PCM) [27,28].

Both in vacuum and solution, the molecular geometries considered have been fully optimized. All calculations have been carried out with the GAMESS package [29]. The representation and analysis of the tridimensional structure of the K^+ channel α-subunit was performed with RasMol version 2.7.2. [30]. The atoms-in-molecules theory was applied with the Morphy98 package [31].

3. Results and discussion

3.1. Identification of putative nucleophilic groups in the receptor site

Analysis of the structure of the α-subunit of the K^+ channel, and specifically of the pore, can be useful for getting insight on the placement and possible nature of the receptor site for aminopyridines. Thus, we have considered the X-ray structure of the KcsA K^+ channel determined by Zhou et al. [19], and deposited in the Protein Data Bank with access code 1J95.

The amino acid sequence for one of the subunits of the tetramer in the α-subunit is shown in Fig. 2. Representing and analyzing the three-dimensional structure of the α-subunit, we find that the pore can be considered to be formed by residues 73–80 and 96–112 (see Fig. 3). The first section, residues 73–80, forms the upper part of the central cavity and the section of the pore going to the extracellular medium. The second sequence, residues 96–112, corresponds to the section of the pore between the cytoplasm and the upper part of the central cavity.

After examining the amino acid sequence in Fig. 2, we found four acidic amino acids. These are placed at positions 51, 71, 118 and 120. All of these are glutamic acid residues (one letter code E). No aspartic acid residues (one letter code B) appear in the structure. A comparison of Figs. 2 and 3 shows that no acidic residues are found into the pore. The closest acidic residue is Glu71, which is placed totally out of the pore surface; see Fig. 3. On the other hand, residues 118 and 120 are placed in the cytoplasmic side (see Fig. 3), just in

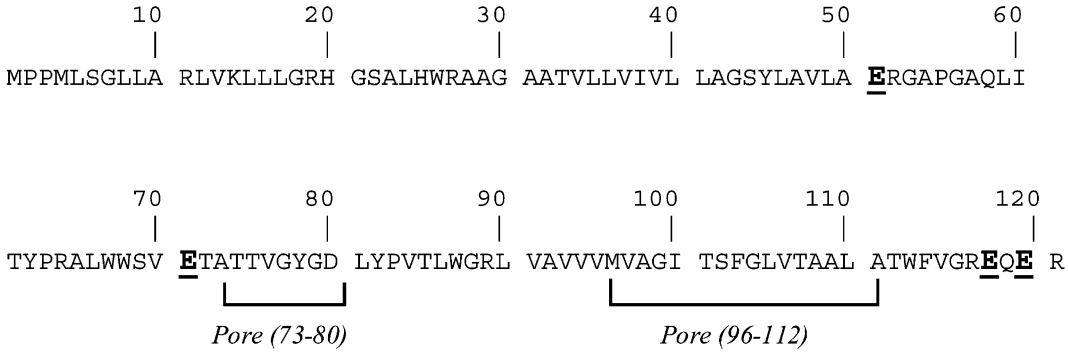

Fig. 2. Amino acid sequence for one of the subunits conforming the tetrameric α-subunit of the K^+ channel. Glutamic acid residues (one letter code E) are represented in bold and underlined.

the lateral entrance of the pore. These results show that the interaction of aminopyridines with a nucleophilic carboxylic residue can only take place outside of the pore.

Another possibility would be that aminopyridines enter the pore and bind somewhere in the inside. Thus, we compare TBA (which is able to enter the pore) with $4AQH^+$, the largest of our series of compounds. Fig. 4 shows, at the same scale, the structures of TBA, determined at the B3LYP/6-31G(d,p) level, and that of $4AQH^+$ in solution obtained at the B3LYP/6-311G(d,p) level. The data collected in Fig. 4 show that TBA can be considered as a 'sphere' of 6.0 Å in radius. The maximum atom-to-atom distance is 9.1 Å, corresponding to the separation between hydrogens in the terminal CH_3 of the aliphatic chains. In contrast, $4AQH^+$ has a planar structure inscribed in a rectangle of sides 5.7×6.2 Å. The linear dimensions and the volume occupied by $4AQH^+$ are smaller than that of TBA. In addition, we have computed the inner size of the pore when it opens to the cytoplasm. We find a square with a side of 4.5 Å (distance between the methyl carbons of the

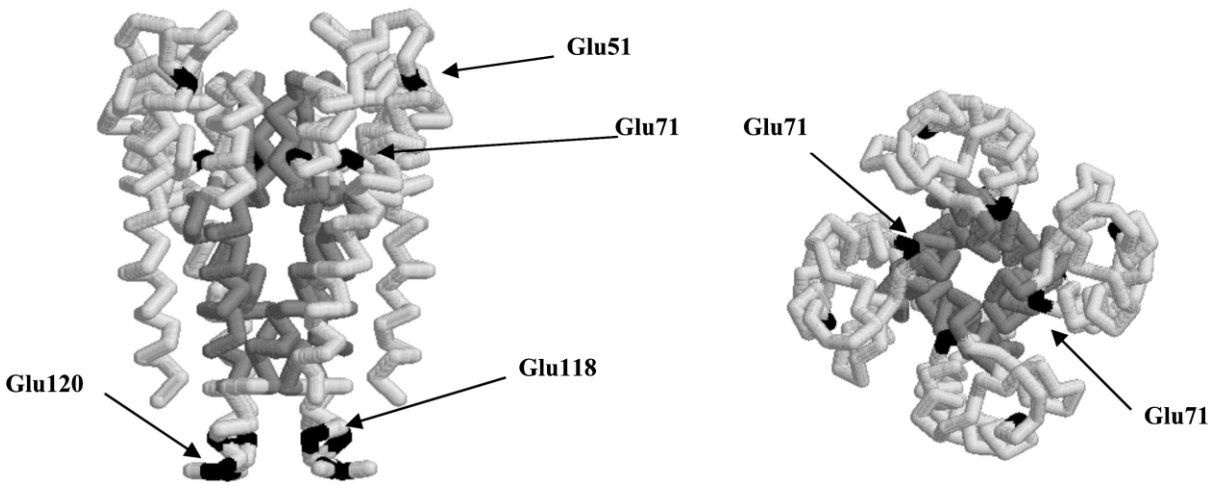

Fig. 3. Three-dimensional structure of the α-subunit of the K^+ channel. To the left, a front image is shown, whereas to the right we have an upper view from the extracellular side. The channel is shown in gray. Acidic residues are shown in black and identified by residue number.

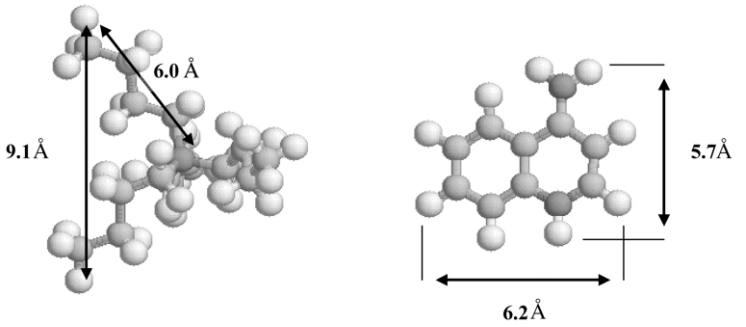

Fig. 4. Structures of TBA and $4AQH^+$. The scale is the same in both cases.

Val 115 residues), which define a diagonal of 6.4 Å. From these data, we can conclude that $4AQH^+$ is able to enter the pore. Since the rest of aminopyridines in our series are smaller than $4AQH^+$, all of them can enter the pore.

The X-ray data [19] show that TBA enters the pore from the cytoplasmic side of the channel, reaching the large central cavity. However, TBA is not able to exit the pore since the section between the central cavity and the extracellular medium is very narrow. The upper zone of the central cavity is analyzed considering the amino acid sequence collected in Fig. 2, and the three-dimensional structure of the α-subunit. We find that, in this zone, the mouth of the pore is formed by residues Thr74–Thr75–Val76. The structure has a π-electronic character due to the presence of the double C=O bonds and the peptide bonds for the four Thr74–Thr75–Val76 chains corresponding to the tetrameric structure. Analysis of the pore structure between the cytoplasm and the central cavity, residues 96–112, also shows some π-electronic zones corresponding to C=O groups and peptide bonds. All these groups are susceptible of hydrogen bonding. However, its π-electronic character suggests the possibility of a nucleophilic cation–π interaction between the receptor site and the aminopyridines. This possibility has been proposed by other authors as an explanation for ion selectivity in K^+ channels [32].

No structural change seems to be involved in the blocking of the K^+ channel. In particular, the experimental data show that when the pore is blocked by TBA, the observed structural change in the pore is negligible [19]. Under these conditions, the in vitro activity is determined by the interaction energy with the receptor.[1] Thus, to analyze the role played by the positive charge in the binding to the receptor, we will determine the interaction energy for the two possibilities previously determined: the nucleophilic interaction with a carboxylic group, and with a pure π-electronic system.

3.2. Orientation of nucleophilic groups

To determine the possible orientation of a nucleophile with respect to the positively charged aminopyridines, molecular electrostatic potentials (MEP) can be useful. The electrostatic potential at a point represents the work done to bring a unit positive charge from infinity to that point. This electrostatic component is just one component of the total interaction energy for a complex. The full interaction energy will also include the polariza-

[1] C. Muñoz-Caro and A. Niño, unpublished results. A functional model relating the in vitro activity of aminopyridines with the pK_a and the interaction energy has been developed. Considering that the in vitro activity index is defined as the concentration of neutral aminopyridine needed to produce the same effect on a single neuron, the treatment shows that there are two factors determining this activity index: the protonation ability (i.e. the pK_a) and the affinity for the receptor (ΔG). Since the macromolecular structure does not change, the entropic contribution is small and can be considered constant along the series of compounds. Thus, the Henderson–Hasselbalch equation shows that the activity index (concentration) depends linearly on the acidic constant, K_a, whereas statistical thermodynamics shows an exponential dependence on the interaction energy.

tion, exchange, charge transfer and mixing terms, as classically proposed by Morokuma [33]. However, MEP defines what an approaching system 'sees' at large distance.

It has been shown that the MEP is useful in predicting the orientation of approaching electrophiles [34,35]. The situation for nucleophiles is different since the most positive values are found around the atomic nuclei. These zones of positive potential correspond to the concentrated nature of the nuclear charges [36]. However, useful information about the orientation of an approaching nucleophile can be obtained from the MEP, as illustrated by Politzer et al. [36]. In the present work, to prevent the masking effect of the nuclear charge concentration, we will consider three-dimensional distributions of the MEP around each considered molecule. The MEP can be especially useful in determining the orientation of approaching groups for charged species. Here, the electrostatic component of the interaction energy can be expected to be particularly important [34].

The considered aminopyridines are fully optimized in solution. As previously shown [16], the molecules are co-planar except for 3,4 DiAPH$^+$, which exhibits a little distortion of the two amine groups. The MEPs are determined at the equilibrium geometries.

Fig. 5 shows for the most active compound, 3,4 DiAPH$^+$, the MEP distribution on the molecular plane and planes parallel to this at 2.0 and 4.0 Bohrs, respectively. In the molecular plane, the most positive zone is localized at the atomic nuclei with values as high as 31.81 a.u. However, analyzing the diagrams for 2.0 and 4.0 Bohr, we observe that the most positive zone is delocalized around the aromatic ring, with maximum values of 0.28 and 0.14 a.u., respectively. The effect is that when we separate from the molecular plane, the highest electropositive zone is progressively localized around the pyridinic N–H bond (see, for instance, the evolution of the 0.14-a.u. isocontour line in Fig. 5). These results can be compared with the MEP obtained in solution by Peradejordi et al. [15]. These MEPs were determined at the CNDO/2 level for the considered series of protonated aminopyridines in a plane situated 0.9 Å (1.7 Bohrs) above the molecular plane. We observed a similar distribution of electrostatic potential, with the aromatic rings surrounded by a positive potential zone.

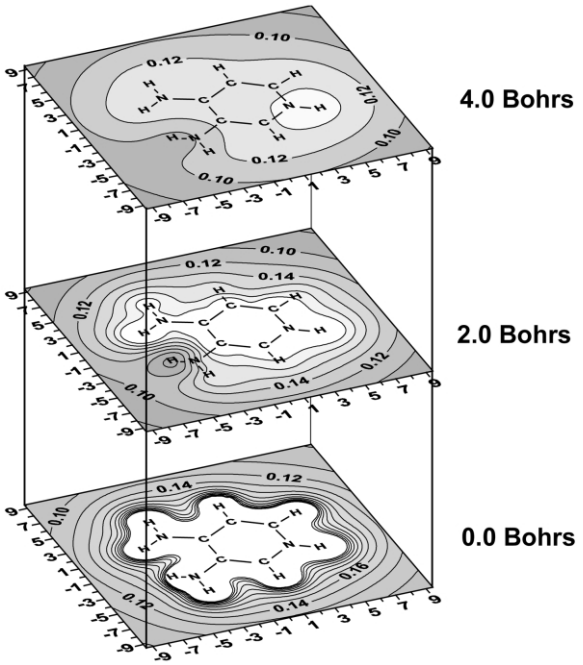

Fig. 5. Three-dimensional distribution of the molecular electrostatic potential for 3,4 DiAPH$^+$. Three isocontour diagrams are shown for planes at 0.0, 2.0 and 4.0 Bohrs of the molecular plane. All data in atomic units (a.u.). Interval between isocontour lines, 0.02 a.u. Clear zones correspond to more positive values.

However, our data for the 4.0-Bohrs plane show that the positive zone is progressively localized around the N–H bond. Therefore, at a large distance, there is a preferred orientation for an approaching nucleophile.

To determine if the previous behavior is general for our series of aminopyridines, we have computed the MEP for the full series on a plane 4.0 Bohrs above the molecular plane (see Fig. 6). For 2APH$^+$, 3APH$^+$, 4APH$^+$ and 3,4 DiAPH$^+$, the most electropositively charged zone is always localized around the N–H bond. For 4AQH$^+$, the most positive zone also involves the pyridinic N–H bond. However, this zone still surrounds part of the pyridinic ring. This effect can be attributed to the π-electronic system of the neighboring ben-

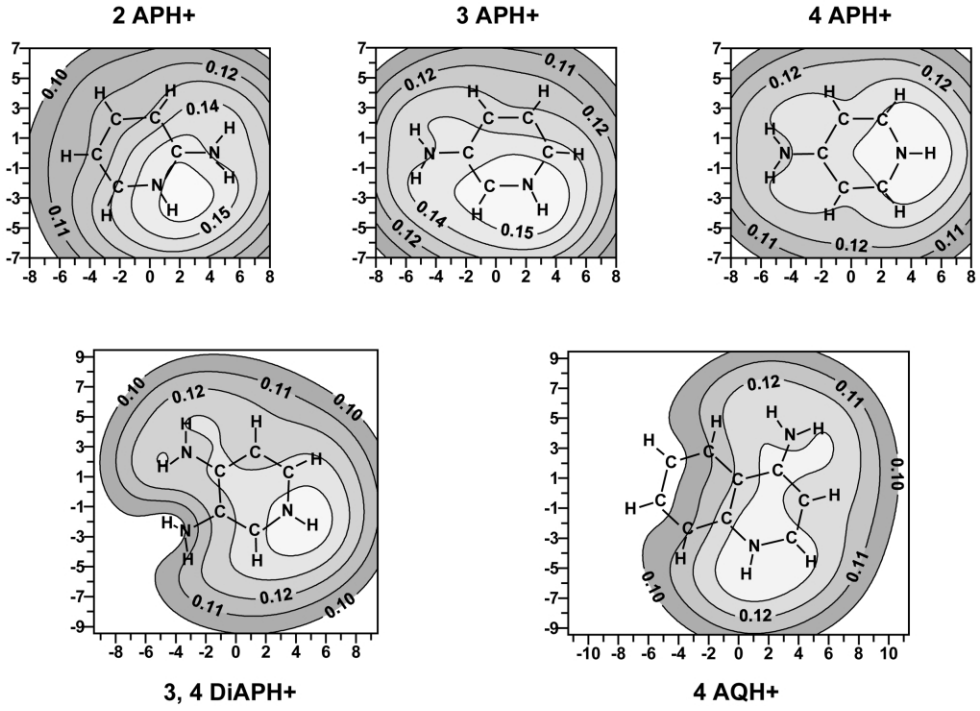

Fig. 6. Isocontour maps of molecular electrostatic potential for the considered series of aminopyridines at a plane placed 4.0 Bohrs above the molecular plane. All data in atomic units (a.u.). Interval between isocontour lines, 0.01 a.u. Clear zones correspond to more positive values.

zene ring. In all cases, the interaction energy in the most positive isocontour line ranges between 0.13 and 0.16 a.u. (81.6–100.4 kcal mol^{-1}). These results show that an approaching nucleophile will be oriented toward the protonated nitrogen on the ring.

3.3. Ionic interaction

To study the ionic interaction of APH^+ with an acidic residue, we constructed a model using a carboxylic group, $HCOO^-$. Initially, the $HCOO^-$ residue is placed with one of its oxygens at a distance of 2 Å from the proton on the pyridinic nitrogen. After relaxation, in vacuum and solution, we found a planar structure for all the complexes. In all cases, we observed a proton transfer from the nitrogen to the carboxylate group. The final complexes were formed by a neutral aminopyridine linked by a hydrogen bond from the pyridinic nitrogen to the acid group. This hydrogen bond can be characterized using Bader's Atoms-in-Molecules Theory (AIM) [37,38]. AIM shows that, at equilibrium, two bonded atoms are connected by a bond path, or Atomic Interaction Line (AIL). The AIL links the nuclei and on it the charge density, ρ, is a maximum. On the AIL lies the Bond Critical Point (BCP), which is a second order saddle point in ρ where the electronic density reaches its maximum along the AIL. The value of ρ at the BCP, ρ_a, is correlated with the concept of bond order, with higher values corresponding to stronger bonds [37,38]. In addition, the sign of the Laplacian of the charge density at the BCP, $\nabla^2\rho_a$, defines the kind of interaction responsible for the bonding [37,38]. A negative sign implies a shared interaction, where the electronic charge is shared by the two nuclei, as in a covalent bond. On the other hand, a positive sign corresponds to a closed-shell interaction, where the electronic charge is concentrated around each nucleus. This is the typical case for ionic or hydrogen bonds.

Table 1
Values in vacuum for the electron density, ρ, and its Laplacian, $\nabla^2\rho$, at the bond critical point for the bond between the proton on the charged aminopyridines and the HCOO– or $CH_2{=}CH_2$ groups

	ρ_a (HCOO–)	$\nabla^2\rho_a$ (HCOO–)	ρ_a ($CH_2{=}CH_2$)	$\nabla^2\rho_a$ ($CH_2{=}CH_2$)
2 APH^+	0.05884	0.09794	0.01382	0.03118
3 APH^+	0.05440	0.10110	0.01587	0.03548
4 AQH^+	0.05484	0.09936	0.01141	0.02639
4 APH^+	0.05336	0.10018	0.01502	0.03420
3,4 $DiAPH^+$	0.05889	0.10052	0.01509	0.03467

Data in atomic units (a.u.).

We apply the AIM theory to our complexes using the one electron density computed in vacuum and solution. In all cases we find an AIL, and its corresponding BCP, connecting the transferred proton and the pyridinic nitrogen. The ρ_a and $\nabla^2\rho_a$ values for the five complexes, in vacuum and solution, are collected in Tables 1 and 2, respectively. The positive sign of $\nabla^2\rho_a$ shows the presence of a closed-shell interaction. In vacuum, the values of ρ_a (approx. 5×10^{-2} a.u.) are typical of a hydrogen bond [37,38], corresponding to a variation of relative bond strength of:

$$3,4\ DiAPH^+ \simeq 2APH^+ > 4AQH^+ \simeq 3APH^+ > 4APH^+$$

In solution, we find the values of ρ_a to be greater than in vacuum, corresponding now to a variation of relative bond strength of:

$$3,4\ DiAPH^+ \simeq 4APH^+ > 4AQH^+ > 3APH^+ > 2APH^+$$

Considering the correspondence between ρ_a and bond orders, in solution, the hydrogen bond in the complexes is stronger than in vacuum. This fact is also observed in the value of the N–H distance. In all cases, this distance is approximately 0.1 Å smaller in the complexes in solution than in vacuum. A very interesting fact is that the strength of the hydrogen bond in solution correlates with the in vitro activity variation; see Table 2.

To analyze the variation of interaction energy, total energy values for our series of aminopyridines and for the complexes, in vacuum and aqueous solution, are collected in Table 3. The relative interaction energy, $\Delta\Delta E$, is determined as the difference between the total energy for the complexes and the isolated aminopyridines, referred to the less stable complex (lsc):

$$\Delta\Delta E_i = \Delta E_i - \Delta E_{lsc}$$

where

$$\Delta E_i = E_i^{complex} - E_i^{APH+}$$

Since the different ΔE values correspond to the same receptor, we can expect a very small effect of the basis set superposition error (BSSE) on $\Delta\Delta E$. Using the Boys and Bernardi counterpoise method [40], the BSSE is determined for the series of aminopyridines using the structure found in the complexes. Maximum/minimum BSSE are found

Table 2
Values in solution for the electron density, ρ, and its Laplacian, $\nabla^2\rho$, at the bond critical point for the bond between the proton on the charged aminopyridines and the HCOO– or $CH_2{=}CH_2$ groups

	ρ_a (HCOO–)	$\nabla^2\rho_a$ (HCOO–)	ρ_a ($CH_2{=}CH_2$)	$\nabla^2\rho_a$ ($CH_2{=}CH_2$)
2 APH^+	0.06031	0.09734	0.01112	0.02687
3 APH^+	0.06556	0.09329	0.01331	0.03249
4 AQH^+	0.07368	0.08585	0.00997	0.02439
4 APH^+	0.07362	0.08468	0.00887	0.02125
3,4 $DiAPH^+$	0.07660	0.08338	0.01217	0.03000

Data in atomic units (a.u.).

Table 3
Total energy (in atomic units) for the isolated aminopyridines and the complexes considered

	APH^+ (vacuum)	APH^+ (solution)	HCOO− (vacuum)	HCOO− (solution)	$CH_2{=}CH_2$ (vacuum)	$CH_2{=}CH_2$ (solution)
2 APH^+	−303.928677	−304.016474	−493.309529	−493.320193	−382.497329	−382.576924
3 APH^+	−303.920724	−304.007166	−493.293601	−493.308578	−382.490184	−382.568254
4 AQH^+	−457.526515	−457.605661	−646.882516	−646.899803	−536.093446	−536.166715
4 APH^+	−303.936606	−304.021919	−493.298939	−493.315860	−382.503900	−382.582529
3,4 $DiAPH^+$	−359.282905	−359.367429	−548.640709	−548.657617	−437.848304	−437.928886

Results obtained after full geometry optimization at the B3LYP/6-311G(d,p) level. HCOO− and $CH_2{=}CH_2$ refer to the groups used to form the complexes.

to be 0.26/0.15 kcal mol^{-1} for $2APH^+/3APH^+$, respectively. The maximum effect on $\Delta\Delta E$ is as small as 0.11 kcal mol^{-1}. Thus, the BSSE is neglected in our calculations.

Fig. 7a collects the $\Delta\Delta E$ results. Three cases are considered: the case with the aminopyridines and the complexes in vacuum (pure vacuum case), and two cases where the aminopyridines are considered to be in solution. In the first of these two cases, the complexes are considered in vacuum (limiting case of desolvation), whereas in the other, the complexes are in solution. The pure vacuum case shows the minimum interaction energy for $4AQH^+$. In all cases, however, the general trend is a decrease of the interaction energy with the in vitro activity. This is the opposite behavior to what we expected, considering the interaction energy as a measure of affinity for the receptor. Fig. 7a also shows that the effect of solvation is a small decrease of $\Delta\Delta E$, while the general trend is maintained. Thus, on energetic terms, interaction with an $HCOO^-$ group is not consistent with the observed activity variation.

On the other hand, the proton transfer from the aminopyridine to the carboxylic residue implies a loss of symmetry. As previously shown through the Laplacian of the charge density, $\nabla^2\rho$ [16], the protonated aminopyridines are equivalent from a reactive point of view as long as they retain the proton. Loss of the proton is reflected in a non-

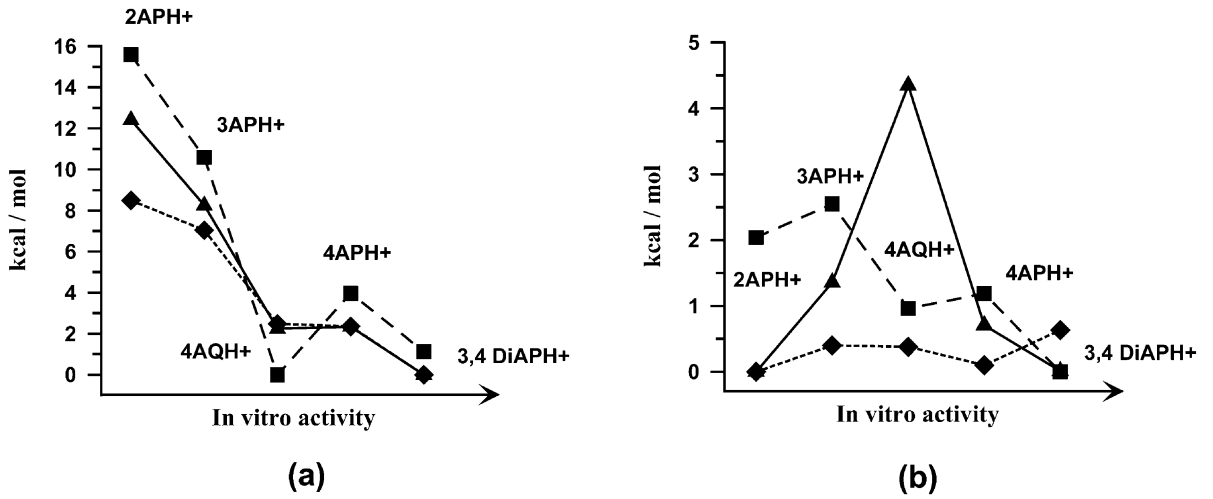

Fig. 7. Relative interaction energy ($\Delta\Delta E$) in kcal mol^{-1} for the supermolecular complexes vs. the observed in vitro activity. Case (a), complexes with $COOH^-$. Case (b), complexes with $CH_2{=}CH_2$. Continuous line: APH^+ in solution, complexes in vacuum. Dotted line: APH^+ and complexes in solution. Dashed line: APH^+ and complexes in vacuum (pure vacuum case).

equivalent distribution of $\nabla^2\rho$, which means a different chemical behavior.

Finally, with respect to the interaction with an acidic residue, it is important to realize that only residues Glu118 and Glu120 are appropriate for binding. In the case of interaction with one of them, only one of the lateral openings of the pore to the cytoplasm will be blocked. Due to the C_4 symmetry of the α-subunit, another three openings remain in the cytoplasmic side. Thus, blocking of the K^+ channel would need the simultaneous fixing of four APH^+ to the four lateral openings.

3.4. Cation–π interaction

As previously shown, the analysis of the X-ray structure of the KcsA K^+ channel [19] suggests the possibility of a cation–π binding being involved in the interaction with the receptor site. To test this possibility, we have used an ethylene group, $CH_2{=}CH_2$, to simulate a pure cation–π interaction. This group is placed on the APH^+ molecular plane with both carbons situated at 3.0 Å of the proton on the pyridinic ring. The total energy results obtained after full molecular relaxation in vacuum and solution are collected in Table 3.

As for the carboxylic residue, the interaction between aminopyridines and the $CH_2{=}CH_2$ is characterized by applying the AIM theory to the one electron density computed in vacuum and solution. In all the complexes we find an AIL, and its corresponding BCP, connecting the proton on the pyridinic nitrogen of the APH^+ and one carbon of the $CH_2{=}CH_2$ group. The ρ_a and $\nabla^2\rho_a$ values for the complexes, in vacuum and solution, are collected in Tables 1 and 2, respectively. We find a positive sign for $\nabla^2\rho_a$, corresponding to a closed-shell interaction. This fact is in agreement with a cation–π interaction, which has electrostatic and quadrupolar components [32]. In vacuum, the values of ρ_a (approx. 10^{-2} a.u.) are smaller than for the hydrogen bonds (approx. 4–5 times smaller), corresponding to a weaker bond and to a relative variation of bond strength of:

$$3APH^+ \simeq 3{,}4\ DiAPH^+ \simeq 4APH^+ > 2APH^+ > 4AQH^+$$

In solution, the magnitude of ρ_a is close to, but smaller than, the values in vacuum. Now, the corresponding relative variation of bond strength is:

$$3APH^+ > 3{,}4\ DiAPH^+ > 2APH^+ > 4AQH^+ > 4APH^+$$

Again, the energetic component is considered by computing relative interaction energies, $\Delta\Delta E$. The BSSE is determined as for the complexes with $HCOO^-$. Maximum/minimum BSSE are found to be 0.15/0.09 kcal mol^{-1} for $4APH^+/4AQH^+$, respectively. The maximum effect on $\Delta\Delta E$ is 0.06 kcal mol^{-1}. Again, due to its small value the BSSE is neglected.

Fig. 7b collects the results for $\Delta\Delta E$. In the pure vacuum case, we observe a behavior similar to that of the carboxylic complexes. For the complexes in vacuum, interaction energy increases along the series, reaching a maximum for $4AQH^+$ (approx. 4.5 kcal mol^{-1}). Afterwards, $\Delta\Delta E$ decreases to values similar to the initial ones in the series. The variation, again, does not correspond to the variation in activity. In contrast with the carboxylic complexes, the behavior for complexes in solution is very different. The interaction energy is greatly reduced (the maximum value is 0.63 kcal mol^{-1} for the 3,4 $DiAPH^+$), and the $\Delta\Delta E$ variation is close to the observed variation of in vitro activity. However, these energetic values are so small that they can be overcome even by the thermal energy, kT, factor 0.59 kcal mol^{-1} at 25 °C. Since in the pore the APH^+ can be partially hydrated, we will have a situation intermediate between the vacuum and fully hydrated results. Anyway, the $\Delta\Delta E$ values can be considered to be small.

In the light of the previous results for the carboxylic and ethylene groups, the positive charge cannot be considered to be mainly responsible for the observed variation in activity. Thus, the second pharmacophoric component (NH_2 groups) should play an at least equally important role through its hydrogen bonding capacity. The typical magnitude of a hydrogen bond is approximately 5 kcal mol^{-1}. Therefore, to reproduce the observed in vitro activity, a receptor site bearing a carboxylic residue implies the overcoming of an interaction

energy of approximately 8–13 kcal mol^{-1}. Thus, it is improbable that one or even two hydrogen bonds can reverse the order of the $\Delta\Delta E$ in the full series to yield the observed variation of activity. Again, these data suggest that the receptor site cannot involve a carboxylic group. On the other hand, only approximately 0.6–4.5 kcal mol^{-1} are involved in the complexes with a $CH_2{=}CH_2$ group; see Fig. 7. These amounts of energy can be easily compensated by the energy variations due to hydrogen bonding. The case is similar to acetylcholine, where its cationic head seems to be involved in a cation–π binding rather than in an ionic one [39].

3.5. Proposed receptor site

Typical K^+ channel blocking agents, such as tetraethylammonium or TBA, act from the inside of the pore. Our structural results show that aminopyridines are sterically able to enter the pore. In addition, we have found that interaction with acidic amino acids, which are placed in the outside of the pore, is difficult to reconcile with the common reactivity pattern and the observed in vitro activity for aminopyridines. Also, our data show that a cation–π interaction is compatible with the hypothesis of hydrogen bonding been responsible for the observed variation of activity.

From these data, one picture emerges, that of a receptor site placed in the inside of the pore bearing a π-electronic component. TBA enters the pore until its reaches the upper part of the large central cavity, where the pore narrows. As shown previously, this zone is formed by residues 74–76. These three residues correspond to the sequence Thr–Thr–Val. Fig. 8a shows the X-ray derived picture of this zone (the hydrogens are not present). We can observe, that threonine 75 has its OH oxygen pointing to the central cavity of the pore. Therefore, due to the C_4 symmetry of the tetramer, four oxygen atoms are oriented to the central cavity. These atoms define a square, with an average side of 3.86 Å, suitable for hydrogen bonding with any of the amine groups, or the proton on the pyridinic nitrogen, of our series of aminopyridines. Around and under this 'bed of oxygens' we find the π-electronic zones corresponding to the C=O groups and to the partial double bond of the peptide bonds for Thr74–Thr75 and Thr75–Val76.

On the other hand, analyzing the section of the pore between the cytoplasm and the central cavity for electronegative groups facing the pore we only found a group formed by four threonine residues (Thr 107), Fig. 8b. The four OH oxygens of these residues define a square with an average side of 6.30 Å. This zone seems appropriate to form several hydrogen bonds involving the amine groups and the protonated nitrogen of APH^+.

These two zones seem to bear the characteristics needed for a receptor site of aminopyridines. To test both possibilities, further work is in progress to develop operative models for these putative receptors.

4. Conclusions

This paper presents a theoretical study of the receptor site for the blocking of voltage dependent K^+ channels by aminopyridines. One of the pharmacophoric characteristics of aminopyridines is the existence of a positive charge. Analysis of the X-ray determined three-dimensional structure of the K^+ channel shows that interaction with a positively charged group can occur in two forms. The first one is an ionic interaction with an acidic residue, which can only take place in the outside of the pore. The second possibility is the internal blocking of the pore in a process involving a cation–π interaction. Supermolecular models were constructed to test both hypotheses.

To determine the orientation of an approaching nucleophile to a charged aminopyridine, we computed molecular electrostatic potential distributions, MEP. It was found that, as we separate from the molecule the most positive zone localizes in the N–H bond of the protonated pyridinic ring. This fact shows that an approaching nucleophile will be oriented toward the proton on the ring.

To test the two interaction possibilities, we constructed two models using a carboxylic group, and for the cation–π case, an ethylene group. We found that interaction with the carboxylic residue leads, in all cases, to a proton transfer from the protonated aminopyridine to the acid group. The

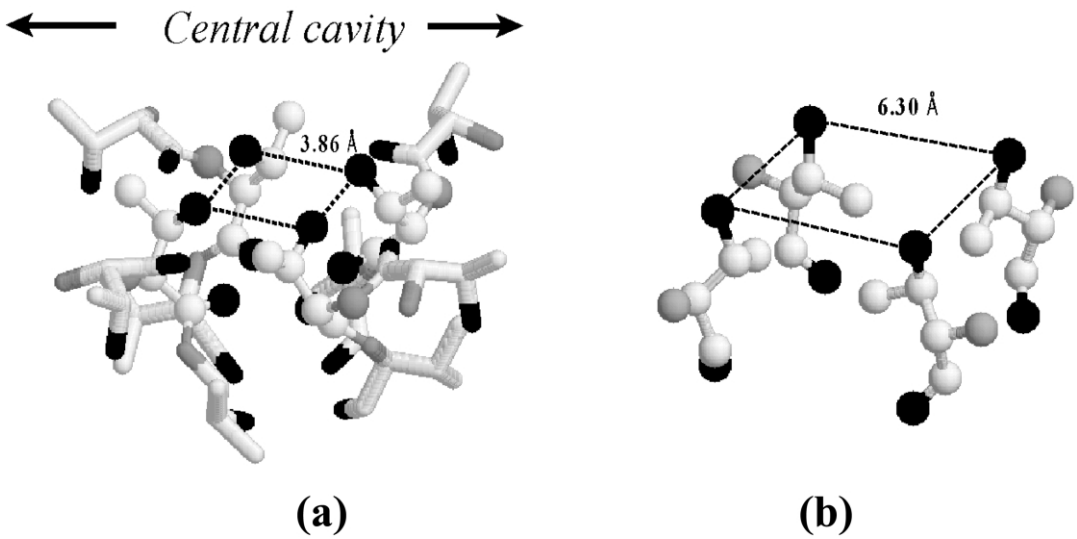

Fig. 8. X-Ray derived structure (lacking hydrogen atoms) for the putative receptor sites in the α-subunit of the KcsA K^+ channel. Case (a), four-fold arrangement of the Thr74–Thr75–Val76 chain in the α-subunit of the KcsA K^+ channel. Thr74 and Val76 are represented as a backbone, whereas Thr75 is represented as a ball-and-sticks model. Case (b), four-fold arrangement of Thr107 within the pore of the channel. Oxygen atoms are shown in black, nitrogen atoms in gray, and carbon atoms in white. The figure shows the squares of four oxygen atoms from the OH group of each Thr.

monomers remain linked by a hydrogen bond. However, the proton transfer leads to a loss of the equivalence of the Laplacian of the electron density field needed for the common reactivity pattern of aminopyridines. In addition, the interaction energy variation ($\Delta\Delta E$), in vacuum and solution, does not agree with the in vitro activity variation. Finally, the C_4 symmetry of the α-subunit of the channel forming the pore shows that, even if aminopyridines bind to one of the acid groups, only one of the four lateral gates to the pore is blocked. All these data do not support the hypothesis of an ionic, cation–anion interaction being involved in the binding to the receptor site.

On the other hand, the AIM theory characterizes a cation–π interaction for the complexes with the ethylene group. Again, in vacuum the $\Delta\Delta E$ variation is not in agreement with the observed activity variation. However, we find that $\Delta\Delta E$ decreases in solution to very small values, with the interaction energy variation approaching the observed variation in activity.

Our data show that the positive charge on the aminopyridines could be involved in a cation–π interaction in the receptor. However, the magnitude of this interaction suggests that the determining factor for the observed in vitro activity variation should be the second pharmacophoric characteristic of aminopyridines: the NH_2 groups able to form hydrogen bonds.

Analysis of the inner zone of the pore, where the channel narrows, shows this zone to be formed by sequence Thr–Thr–Val. Considering that the pore is a tetramer of four α-helices, this zone exhibits rotational (C_4) symmetry. Thus, several π-electronic zones, corresponding to carboxylic groups and peptide bonds, are found. In addition, four oxygens from the OH in the threonine residues are identified pointing to the central cavity of the pore. On the other hand, in the section of the pore between the cytoplasm and the central cavity, we find four electronegative threonine residues with the OH groups facing the pore. From these data, two possible receptor sites can be proposed. The first is defined by four Thr–Thr–Val chains in C_4 symmetry with a 'bed' of four oxygens pointing from the narrow exit channel of the pore to the large central cavity in the channel. The second

corresponds to four Thr residues in the pore, with its four OH groups arranged in a square. Work is in progress to contrast both possibilities.

Acknowledgments

The authors thank the DGESIC (grant # PM98-0073) and the Universidad de Castilla-La Mancha for financial support.

References

[1] G.E. Kirsch, T. Narahashi, 3,4-Diaminopyridine. A potent new potassium channel blocker, Biophys. J. 22 (1978) 507–512.
[2] J. Molgó, M. Lemeignan, F. Peradejordi, P. Lechat, Effects présynaptiques des aminopyridines a la junction neuromusculaire de vertébrés, J. Pharmacol. (Paris) 16 (suppl. II) (1985) 109–144.
[3] C. Carlsson, I. Rosen, E. Nilsson, Can 4-aminopyridine be used to reverse anaesthesia and muscle relaxation?, Acta Anaesthesiol. Scand. 27 (1993) 87–90.
[4] S.R. Schwid, M.D. Petrie, M.P. McDermott, D.S. Tierney, D.H. Maso, A.D. Goodman, Quantitative assessment of sustained-release 4-aminopyridine for symptomatic treatment of multiple sclerosis, Neurology 48 (1997) 817–821.
[5] K.M. McEvoy, A.J. Windebank, N.J.R. Daube, P.A. Low, 3-4-Diaminopyridine in the treatment of Lambert–Eaton myasthenic syndrome, N. Engl. J. Med. 321 (1989) 1567–1571.
[6] J.L. Segal, S.R. Brunnemann, 4-aminopyridine improves pulmonary function in quadriplegic humans with long-standing spinal cord injury, Pharmacotherapy 17 (1997) 415–423.
[7] L.C. Sellin, The action of botulinum toxin at the neuromuscular junction, Med. Biol. 59 (1981) 11–20.
[8] M. Davidson, J.H. Zemishlany, R.C. Mohs, et al., 4-Aminopyridine in the treatment of Alzheimer's disease, Biol. Psychiatry 23 (1988) 485–490.
[9] J.I. Gillespie, O.F. Hutter, The actions of 4-aminopyridine on the delayed potassium current in skeletal muscle fibres, J. Physiol. (Lond.) 252 (1975) 70P–71P.
[10] J. Molgó, H. Lundh, S. Thesleff, Potency of 3,4-diaminopyridine and 4-aminopyridine on mammalian neuromuscular transmission and the effect of pH changes, Eur. J. Pharmacol. 61 (1980) 25–34.
[11] G.E. Kirsch, T. Narahashi, Site of action and active form of aminopyridines in squid axon membranes, J. Pharmacol. Exp. Ther. 226 (1983) 174–179.
[12] J. Molgó, M. Lemeignan, P. Lechat, F. Peradejordi, Increase in evoked transmitter release from motor nerve terminals by some amino *N*-heterocyclic compounds, I, Eur. J. Med. Chem. 20 (1985) 149–153.
[13] J.R. Howe, J.M. Ritchie, On the active form of 4-aminopyridine:block of K^+ currents in rabbit Schwann cells, J. Physiol. 433 (1991) 183–205.
[14] D. Choquet, H. Korn, Mechanism of 4-aminopyridine action on voltage-gated potassium channels in lymphocytes, J. Gen. Physiol. 99 (1992) 217–240.
[15] F. Peradejordi, J. Molgó, M. Lemeignan, Increase in evoked transmitter release from motor nerve terminals by some amino *N*-heterocyclic compounds. II, Eur. J. Med. Chem. 20 (1985) 155–161.
[16] A. Niño, C. Muñoz-Caro, Theoretical analysis of the molecular determinants responsible for the K^+ channel blocking by aminopyridines, Biophys. Chem. 91 (2001) 49–60.
[17] D.A. Doyle, J.M. Cabral, R.A. Pfuetzner, et al., The structure of the potassium channel: molecular basis of K^+ conduction and selectivity, Science 280 (1998) 69–77.
[18] J.M. Gulbis, M. Zhou, S. Mann, R. McKinnon, Structure of the cytoplasmic β subunit-T_1 assembly of voltage-dependent K^+ channels, Science 289 (2000) 123–127.
[19] M. Zhou, J.H. Morais-Cabral, S. Mann, R. McKinnon, Potassium channel receptor site for the inactivation gate and quaternary amine inhibitors, Nature 411 (2001) 657–661.
[20] S.G. Stepanian, I.D. Reva, E.D. Radchenko, L. Adamowicz, Conformational behavior of α-alanine. Matrix-isolation infrared and theoretical DFT and ab initio study, J. Phys. Chem. A 102 (1998) 4623–4629.
[21] M. Lozynski, D. Rusinska-Roszak, H.-G. Mack, Hydrogen bonding and density functional calculations: The B3LYP approach as the shortest way to MP2 results, J. Phys. Chem. A 102 (1998) 2899–2903.
[22] A. Niño, C. Muñoz-Caro, M.L. Senent, Suitability of different levels of theory for modelling of hydroxamic acids, J. Mol. Struct. THEOCHEM 530 (3) (2000) 291–300.
[23] R. Krishnan, J.S. Binkley, R. Seeger, J.A. Pople, Self-consistent molecular orbital methods. XX. A basis set for correlated wave functions, J. Chem. Phys. 72 (1980) 650–654.
[24] A. Niño, C. Muñoz-Caro, D.C. Moule, Wagging and torsion vibronic structure in the $T_1 \leftarrow S_0$ electronic spectrum of acetaldehyde, J. Phys. Chem. 98 (1994) 1519–1524.
[25] A. Niño, C. Muñoz-Caro, D.C. Moule, Three-dimensional vibrational study of the coupling between the methyl torsion and the molecular frame in the S_0 state of acetaldehyde, J. Phys. Chem. 99 (1995) 8510–8515.
[26] A. Niño, C. Muñoz-Caro, Effect of large-amplitude vibrations on the thermodynamics of malondialdehyde, J. Phys. Chem. A 102 (1998) 1177–1180.
[27] M. Cossi, V. Barone, R. Cammi, J. Tomasi, Ab initio study of solvated molecules: a new implementation of the polarizable continuum model, Chem. Phys. Lett. 255 (1996) 327–335.

[28] V. Barone, M. Cossi, J. Tomasi, A new definition of cavities for the computation of solvation free energies by the polarizable continuum model, J. Chem. Phys. 107 (1997) 3210–3221.
[29] M.W. Schmidt, K.K. Baldridge, J.A. Boatz, et al., General atomic and molecular electronic structure system, J. Comput. Chem. 4 (1993) 1347–1363, Version: June 2001..
[30] Based on RasMol by Roger Sayle. Version 2.7.0 March 1999, 2.7.1 June 1999, 2.7.2 August 2000 by Herbert J. Bernstein 1998–2000
[31] MORPHY98, a topological analysis program written by P.L.A. Popelier with a contribution from R.G.A. Bone, UMIST, Manchester, England, EU (1998)
[32] J.C. Ma, D.A. Dougherty, The cation–π interaction, Chem. Rev. 97 (1997) 1303–1324.
[33] K. Morokuma, Why do molecules interact? The origin of electron donor–acceptor complexes, hydrogen bonding, and proton affinity, Accounts Chem. Res. 10 (1977) 294–300.
[34] E. Scrocco, J. Tomasi, Electronic molecular structure, reactivity and intermolecular forces: an heuristic interpretation by means of electrostatic molecular potentials, Adv. Quantum Chem. 11 (1978) 115–193.
[35] A.R. Leach, Molecular Modelling. Principles and Applications, Prentice-Hall, 2001.
[36] P. Politzer, S.J. Landry, T. Warnheim, Proposed procedure for using electrostatic potentials to predict an interpret nucleophilic processes, J. Phys. Chem. 86 (1982) 4767–4771.
[37] R.F.W. Bader, Atoms In Molecules. A Quantum Theory, Oxford University Press, 1995.
[38] P. Popelier, Atoms In Molecules. An Introduction, Prentice Hall, 2000.
[39] G.L. Patrick, An Introduction to Medicinal Chemistry, Oxford University Press, 1997, pp. 215–216.
[40] S.F. Boys, F. Bernardi, The calculation of small molecular interactions by the differences of separate total energies. Some procedures with reduced errors, Mol. Phys. 19 (1970) 553–566.